Glycosylated copper(II) ionophores as prodrugs for â-glucosidase activation in targeted cancer therapy.

Glycosylated copper(II) ionophores as prodrugs for β-glucosidase activation in targeted cancer therapy
Valentina Oliveri, Maurizio Viale, Giulia Caron, Cinzia Aiello, Rosaria Gangemi and Graziella Vecchio
Dalton Trans., 2013,42, 2023-2034
DOI: 10.1039/C2DT32429F
First published online 06 Nov 2012

Glycosylated prodrugs of oxines for enzyme-specific activation in targeted cancer therapy

Valentina Oliveri[1], Maurizio Viale[2], Giulia Caron[3], Cinzia Aiello[2], Rosaria Gangemi[2] and Graziella Vecchio[1*]

[1] *University of Catania, Dipartimento di Scienze Chimiche, Viale A. Doria, 6, 95125 – Catania.*

[2] *IRCCS Azienda Ospedaliera Universitaria San Martino – IST Istituto Nazionale per la Ricerca sul Cancro, U.O.C. Terapia Immunologia, L.go R. Benzi, 10, 16132 – Genova.*

[3] *University of Torino, BMSS, Via Quarello, 11, 10135 – Torino*

*** To whom correspondence should be addressed**: phone, +39 0957385064; Fax: +39 095580138; Email: gr.vecchio@unict.it.

Abstract

8-Hydroxyquinoline derivatives are metal-binding compounds that have recently awakened interest as therapeutic agents for cancer therapy. In this scenario, we designed and synthesized three new glucoconjugates, 5,7-dichloro-8-quinolinyl-β-D-glucopyranoside, 5-chloro-8-quinolinyl-β-D-glucopyranoside and 2-methyl-8-quinolinyl-β-D-glucopyranoside and investigated their biological properties in comparison to the parent 8-hydroxyquinoline derivatives. Our *in vitro* data show that 2 out of 3 glycosilated compounds possess a pharmacologically-relevant antiproliferative activity against tumor cells, similar to that of their parent compounds; this activity is associated with a relevant triggering of apoptosis. The pharmacological profile of the investigated compounds depends on the cellular enzymatic β-glucosidase activity, as demonstrated by the inhibition of antiproliferative activity in the presence of the 2,5-dideoxy-2,5-imino-D-mannitol.

Introduction

Cancer, the uncontrolled and pathological proliferation of abnormal cells, is the second leading cause of human death after cardiovascular diseases in developing, as well as advanced, countries.[1,2] Although there are many therapeutic strategies, including chemotherapy and radiotherapy, high systemic toxicity and drug resistance limit the successful outcomes in most cases. Therefore, novel treatments are urgently needed for cancer therapy.

8-Hydroxyquinoline derivatives (OHQs) are metal-binding compounds that have recently been viewed with interest as therapeutic agents for cancer and Alzheimer disease (AD) [3]. Clioquinol (5-chloro-7-iodo-8-hydroxyquinoline, CQ) is the most known member of this family. In the 1950s, it was widely used as an amebicide for the treatment of diarrhea[4]. CQ has widely been investigated as a metal-protein-attenuating compound. It also reached clinical trials for the treatment of AD disease, but clinical studies have been interrupted due to issues with the purity of large-scale CQ production: small amount of di-iodo-8-hydroxyquinoline, known carcinogen, contaminated CQ production. Currently, CQ is in phase I clinical trial in patients with hematologic malignancy, such as leukemia, myelodysplasia, non-Hodgkin's and Hodgkin's lymphomas, and multiple myeloma.[5]

The anticancer mechanism of OHQs is related to the complexation of copper ions[6]. This transition metal ion is involved in many different cellular mechanisms: as cofactor for different Cu-dependent oxidases in respiration processes and in other proteins.[7] Even if copper homeostasis is tightly regulated, elevated copper level have been found in many types of cancer. Although its accumulation in cancer cells has not yet been fully explained, it is conceivable that Cu^{2+} may help the tumor in its growth and release of metastatic cells. In particular, Cu^{2+} is necessary for angiogenesis,[8,9] that is the mechanism by which the tumor may survive and grow beyond one or two millimeters of diameter. The need for Cu^{2+} ions by tumor cells justified the clinical use of specific Cu^{2+} chelators as anticancer agents [10,11,12]. It is important to note that the use of Cu complexes as cancer therapeutics is likely dependent more on their cytotoxic action, rather than modulation of Cu homeostasis.[13] Although the mechanism of action is not completely understood, experimental

evidence suggests that OHQs and CQ act as anticancer agents as 20S proteasome inhibitors in the presence of copper(II).[14,15] Other mechanisms have been reported to explain the cytotoxicity of CQ, such as induction of the cytoplasmatic clearance of X-linked inhibition of apoptosis protein[16] and induction of DNA double strand-breaks.[17]

The crucial role played by Cu^{2+} ions in many cellular mechanisms also explains how an uncontrolled depletion of Cu^{2+} could be the cause of toxic events. For this reason, unselective chelation of essential metal ions due to an anticancer treatment could have severe side effect and should therefore be avoided. A well-accepted strategy to prevent these side effects from occurring consists in using prodrugs.

In very general terms, prodrug design aims to overcome a number of limitations of drug candidates:[18] a) pharmaceutical problems, such as poor solubility, insufficient chemical stability, unacceptable taste or odor, and irritation or pain; b) pharmacokinetic problems, such as insufficient oral absorption, inadequate blood-brain barrier permeability, marked pre-systemic metabolism, and toxicity; and c) pharmacodynamic problems, such as low therapeutic index and lack of selectivity at the site of action.

For cancer therapy, glucose-conjugated prodrugs are of great interest since they can enhance uptake of a drug in cancer cells, as tumor cells require a significant amount of glucose. In fact the efficiency of ATP production in normal cells does not satisfy the high energy requirements of cancer cells and thus glucose transporters (GLUTs) are overexpressed in cancer cells to improve glucose uptake.[19] The ratio of GLUTs expression in malignant versus normal cells is about 100-300.[20]

Once delivered to the target tissue, non-cytotoxic prodrugs require tumor-specific activation. This may occur by the hypoxic environment of solid tumors, by the tumor-associated proteases or by the enzymes selectively present in the tumor. Prodrug monotherapy is a convenient strategy to activate prodrugs using an enzyme already present in the tumor. In particular, appropriate glycosylated prodrugs are activated by β-glucosidase overexpressed in tumor cells.[21]

Summing-up, glycosylated prodrugs of copper-binding compounds such as OHQs could combine a selective delivery to tumor tissues with a tumor specific mechanism of activation and specific antitumor activity and therefore could represent a new strategy for the research of anticancer agents. In addition the presence of the sugar unit prevents copper(II) binding and could prevent the systemic undesired complexation. Moreover, glycosylated prodrugs of OHQs are expected to be more soluble than corresponding parent compounds and therefore more in line with drug-likeness criteria.

In a previous explorative study we showed for the first time the antiproliferative activity of 5-chloro-7-iodo-8-quinolinyl-β-D-glucopyranoside (GluCQ) and for comparison of 8-hydroxyquinoline glucoconjugate (GluOHQ) as new prodrugs[22]. In particular, we observed that these compounds show significant antiproliferative activities against different cancer cell lines in the presence of copper(II). We also hypothesized that the glucose moiety had to be cleaved in cells by the β-glucosidase and then the aglycone was able to complex copper(II) ions. In this paper we describe the synthesis of three new glyconjugates of OHQs (Figure 1) with good physicochemical and ADME profile, the characterization and stability, the chelating properties of copper ions, the *in vitro* anticancer biological profile and, finally, some docking experiments to shed light on experimental results. We clarify some aspects of the action mechanism of the glycosylated derivatives by demonstrating the role of the β-glucosidase enzyme. For comparative purposes, the data for the corresponding 8-hydroxyquinolines were also collected (Figure 1).

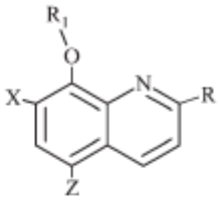

Compound	X	Z	R_1	R
Cl_2HQ	Cl	Cl	H	H
ClHQ	H	Cl	H	H
MeHQ	H	H	H	CH_3
$GluCl_2HQ$	Cl	Cl	Glucose	H
GluClHQ	H	Cl	Glucose	H
GluMeHQ	H	H	Glucose	CH_3
OHQ	H	H	H	H
CQ	I	Cl	H	H
GluOHQ	H	H	Glucose	H
GluCQ	I	Cl	Glucose	H

Figure 1. Chemical structures of investigated compounds

Results

In silico physicochemical and ADME profile. Lipinski's Rule of Five (Ro5) is a widely accepted rule of thumb to determine if a chemical compound with a certain pharmacological or biological activity has molecular properties (i.e. the molecular weight is over 500 Da, the calculated log P is over 5, the structure includes more than 5 hydrogen-bond donors and more than 10 hydrogen-bond acceptors) that could be associated with poor absorption and distribution properties. Designed compounds (Figure 1) were tested by Ro5. The results revealed that all compounds are within the range set by Ro5 as per Table 1.

Properties included in the Ro5 may vary with molecular flexibility. To check the extent of the influence of flexibility on the 3D structure of the glycosylated prodrugs we monitored lipophilicity, which is widely accepted as the most relevant molecular property associated to biodistribution.[23] In practice, we firstly submitted all prodrugs to a conformational analysis. Then we calculated the log P of any resulting conformer (called virtual log P[24]), the average log P value, and the lipophilicity range (i.e. the difference between the highest and the lowest virtual log Ps). Data in Table 1 show that the influence of molecular flexibility is modest (lipophilicity range lower than 0.5).

Solubility is a key property in drug discovery. In this study, solubility data of investigated compounds are of computational nature and expressed as ALOGpS (the higher, the more soluble the compound, see Experimental Part for more details) and reported in Table 1. They point out that prodrugs are expected to be more soluble than corresponding drugs.

Finally, to predict the ADME behaviour, the compounds under study were projected on the following pre-calculated models implemented in the VolSurf+ software (see Experimental Part for more details): plasma protein affinity (PB), distribution volume (VD), Caco-2 cell permeability (CACO2), blood–brain barrier permeation (lgBB) and metabolic stability (MetStab). The ADME profiles of compounds (Table 1) were evaluated according to the rules proposed by Carosati et al.[25]

Most values are in line with the alert threshold values of drug-likeness. The low absorption predicted by the CACO2 descriptor (0.2 the lowest acceptable threshold) has limited relevance here since absorption is expected to be related to active transport mechanisms.

Table 1. Lipinski's Ro5, lipophilicity, solubility and ADME descriptors of investigated compounds.

	Ro5 descriptors					Lipophilicity		Solubility	ADME descriptors				
Compounds	MW [a]	HBD [a]	HBA [a]	LOGP [a]	Ro5 violation [a]	averaged log P [b]	range [b]	LOGpS [c]	PB [d]	VD [d]	CACO2 [d]	LgBB [d]	MetStab [d]
Cl_2HQ	*214.05*	*1*	*2*	*3.15*	*0*	*Nc [e]*	*Nc [e]*	*-3.19*	*88*	*0.09*	*1.12*	*0.42*	*90*
ClHQ	*179.60*	*1*	*2*	*2.47*	*0*	*Nc [e]*	*Nc [e]*	*-2.33*	*78*	*0.17*	*1.19*	*0.37*	*98*
MeHQ	*159.18*	*1*	*2*	*2.23*	*0*	*Nc [e]*	*Nc [e]*	*-1.95*	*70*	*0.28*	*1.29*	*0.33*	*94*
GluCl_2HQ	376.19	4	7	0.56	0	1.09	0.11	-2.3	29	0.12	-0.47	-1.12	100
GluClHQ	341.74	4	7	-0.05	0	0.54	0.09	-1.87	32	0.14	-0.48	-1.22	100
GluMeHQ	321.33	4	7	-0.29	0	0.76	0.09	-1.69	24	0.21	-0.42	-1.29	100
OHQ	*145.16*	*1*	*2*	*1.83*	*0*	*Nc [e]*	*Nc [e]*	*-1.54*	*66*	*0.17*	*1.17*	*0.29*	*100*
CQ	*289.50*	*0*	*1*	*4.08*	*0*	*Nc [e]*	*Nc [e]*	*-4.09*	*93*	*0.30*	*1.62*	*0.65*	*68*
GluOHQ	307.30	4	7	-0.69	0	-0.04	0.09	Nd [f]	18	0.17	-0.53	-1.31	100
GluCQ	467.64	4	7	0.88	0	1.56	0.11	-2.83	35	0.12	-0.43	-1.13	100

a) Calculated by VolSurf+; definitions: MW= Molecular Weight, HBD = number of hydrogen bond donor groups, HBA = number of hydrogen bond acceptor groups, LOGP = logarithm of the partition coefficient, Ro5 violations = number of violations to the Ro5.

b) Calculated with VEGA ZZ 3.0.0; definitions: averaged log P = averaged log P value calculated using log Ps calculated on the series of conformers (virtual log Ps), range = difference between the largest and the lowest virtual log P values.

c) Calculated by VCCLAB; definition: LOGpS = minus logarithm of the solubility values calculated by the software. A solubility larger than -4 is considered with drug likeness criteria.

d) Calculated by VolSurf+; definitions: PB = percentage of protein binding, VD = distribution volume [l/kg], CACO2 = qualitative value of cells permeability, lgBB = logarithm of the Blood-Brain Barrier distribution, MetStab = percentage of the remaining compound after incubation with human CYP3A4 enzyme. The following drug likeness criteria were used to evaluate data: PB lower than 90%, CACO2 lowest threshold value 0.2; lgBB lower than -0.5 indicate very poor brain penetration, values greater than 0.5 indicate high brain penetration; MetStab greater than 50 indicate stable behaviour.

e) Not calculated. f) Not determined.

Chemistry

Synthetic aspect. The new compounds $GluCl_2HQ$, GluClHQ and GluMeHQ were synthesized by a modified Michael procedure as reported by us[222] for similar compounds (scheme 1). The desired compounds were achieved through a one-pot reaction. Briefly, the quinoline compounds were dissolved in a water/methanol solution of the base K_2CO_3 and then a solution of glycosyl bromide in dichloromethane was added together with a phase transfer catalyst, such as tetrabutylammonium salts. This reaction produced the β-anomer of the glycosides. The pure products were isolated by precipitation. All novel compounds were characterized by ^1H NMR and ^{13}C NMR spectroscopy as well as ESI-MS. NMR spectra confirm the identity of the products.

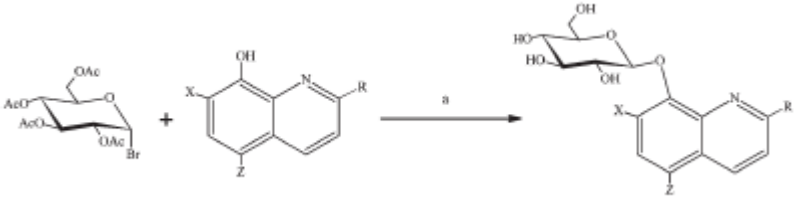

Scheme 1. Reagents and conditions: (a) K_2CO_3(aq), Bu_4NBr,CH_2Cl_2, 68h, r.t.

The ESI spectra of glucoconjugates show at least three peaks due to proton and sodium adduct ion and the dimeric sodium adduct ion. Furthermore, the zoom scan spectra of the halogenated compounds show typical isotopic patterns due to the presence of the halogen atoms.

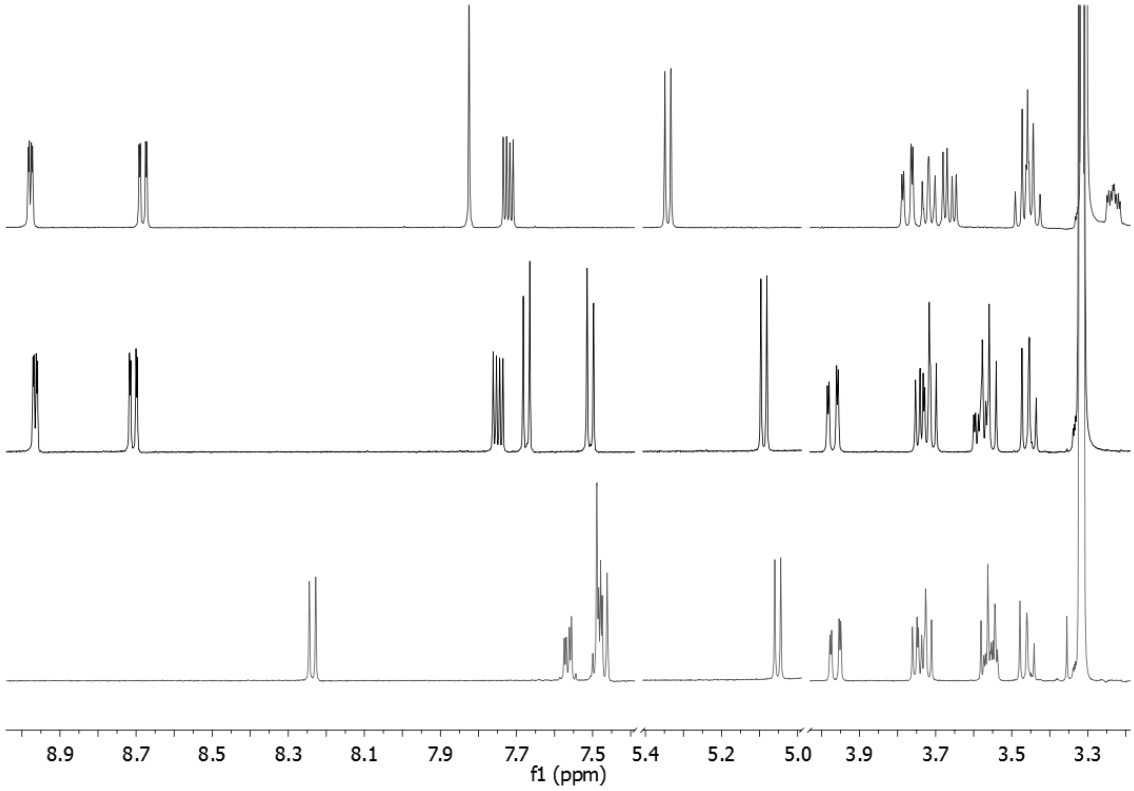

Figure 2. NMR spectra of the glucoconjugates at 500 MHz in MeOD. $GluCl_2HQ$ (up), GluClHQ (middle), MeHQ (down).

The ^1H NMR spectra of glucoconjugates are reported in Figure 2. In all the spectra the signals due to the quinoline moiety and the signals due to the sugar moiety can be seen. The $J_{1,2}$ values of the glucose ring (about 7.8 Hz) confirm the β configuration for all derivatives**.** The H-1 of the glucose moiety is downfield shifted because of the deshielding effect of the aromatic ring as reported for similar compounds and resonates at about 5.1 ppm.[26] The presence of chlorine at C-7 position in $GluCl_2HQ$ further shifts the H-1 downfield at about 5.4 ppm. The glucose protons of $GluCl_2HQ$ are more shifted upfield in comparison to other two glycoconjugates as reported elsewhere for CQ glyconjugates. The disposition of the aromatic ring compared to the sugar unit affects the chemical shifts especially of glucose H-5 and H-6.

CD spectra of the three new compounds (Figure 3) were also recorded in methanol. The presence of the glucose moiety induces chirality in the region of π-π* of the aromatic ring.[27] GluClHQ and GluMeHQ have similar CD spectra that show a slight negative band at 310 nm and a

more intense negative band at 200 nm. The CD spectrum of $GluCl_2HQ$ is significantly different and displays a positive band at 300 nm and two intense negative bands at 240 and 206 nm, respectively. The $\Delta\varepsilon$ values of $GluCl_2HQ$ spectrum are higher than the other two compounds, suggesting a different orientation of the aromatic ring respect to the sugar moiety in this case. This could be due to the presence of 7- substituent (a chlorine atom) given that a similar trend is observed for GluCQ. The CD spectra are perfectly consistent with NMR data.

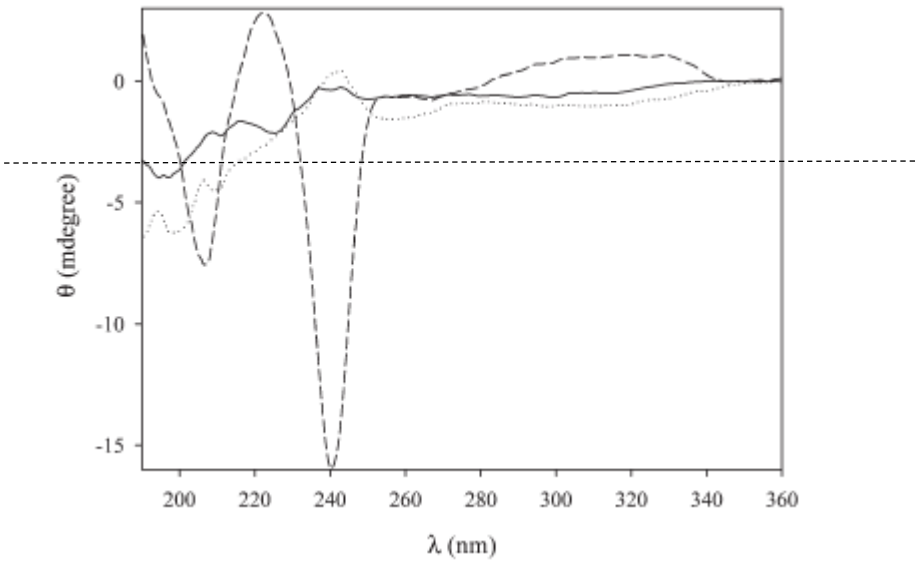

Figure 3. CD spectra of GluMeHQ (—), GluClHQ (...), $GluCl_2HQ$(---) in methanol.

Copper complexes. Copper(II) complexes of some hydroxyquinoline derivatives have been investigated by different techniques.[28] We investigated the coordination properties of MeHQ, ClHQ and Cl_2HQ by ESI-MS. A picture of the metal–ligand complexes formed in solution can be obtained by the mass spectrometric data. The ESI-MS spectra in the positive mode of the hydroxyquinoline derivative solutions containing $CuSO_4$ were recorded. The experiments were carried out at different pH, from 4.0 to 10.0. The formation of complex species was observed for pH > 5. In Table 2 the pseudo-molecular ions of the observed species complexes are reported. The assignments of the peaks in ESI-MS spectra were done by comparing the experimental isotopic patterns with the corresponding simulated profiles. As expected, the three compounds can form

different complex species with copper (II). These data are in agreement with data previously reported in the literature for CQ and other similar compounds[28].

Table 2. ESI-MS characterization of all the $^{63}Cu^{2+}$ complexes $[Cu^{2+}] = [L] = 3.0x10^{-5}$ M. L is a hydroxyquinolinate derivative.

Ligand	Assignment	Calculated (m/z)	Found (m/z)
MeHQ	$[LH+H]^+$	160.1	160.1
	$[CuL+H_2O]^+$	239.0	238.9
	$[CuL_2+H]^+$	380.1	379.9
	$[CuL_2+Na]^+$	402.0	401.9
	$[CuL_2+K]^+$	418.0	418.0
	$[Cu_2L_3]^+$	600.0	599.8
ClHQ	$[LH+H]^+$	180.0	180.1
	$[CuL+H_2O]^+$	292.9	292.8
	$[CuL_2+H]^+$	419.9	419.9
	$[CuL_2+Na]^+$	441.9	441.9
	$[Cu_2L_3]^+$	659.9	659.9
Cl_2HQ	$[LH+H]^+$	214.0	214.0
	$[CuL+H_2O]^+$	274.9	274.9
	$[CuL_2+H]^+$	487.9	487.8
	$[CuL_2+Na]^+$	509.9	487.8
	$[Cu_2L_3]^+$	762.8	762.8

Chemical and enzymatic stability. Chemical stabilities of the investigated compounds (Figure 1) were monitored by several techniques such as mass spectrometry, UV-vis spectroscopy and chromatography.

All glucoconjugates are very stable in the range of pH values (pH 4-11) and temperatures (25-37° C) investigated. No decomposition was detected after 24 hours under these conditions. In

particular, incubation of prodrugs at 37 °C in PBS (phosphate-buffered saline, pH 7.4) revealed that the prodrugs were stable for at least 1 week.

In order to evaluate the ability of prodrugs to release the active moiety in the presence of the specific enzyme, hydrolysis assays were carried out with β-glucosidase and monitored by several techniques, especially UV-vis spectroscopy. Almond β-glucosidase, commercially available, was used as the model enzyme. The UV-vis spectra were recorded at different time points to follow the hydrolysis at pH 7.4. When the glycoconjugates are hydrolized, the OHQ moiety is released and new bands due to the free oxine moiety appear. For comparison the same assay was repeated for the prodrugs in the absence of glucosidase and no modification of the bands was observed. The glucoconjugates showed different behaviour in the presence of β-glucosidase (Figure 4). The glycosidic bond of $GluCl_2HQ$ and GluClHQ was rapidly cleaved (within 40 min), showing that the glucoside trigger is readily accessible by the enzyme, despite the presence of bulky aromatic moieties. Oxine was released significantly faster from $GluCl_2HQ$ and GluClHQ than from GluCQ and GluOHQ. In contrast, GluMeHQ did not show any significative cleavage within 2 hours. However, GluMeHQ was partially cleaved in longer periods of times. Half-lives of prodrugs in the presence of β-glucosidase are reported in Table 3.

Table 3. Half-lives of prodrugs in the presence of almond β-glucosidase ($1.0x10^{-6}$M) at 37°C (pH 7.0).

	$GluCl_2HQ$	**GluClHQ**	**GluMeHQ**	**GluCQ**	**GluOHQ**
$t_{1/2}$ (min)	9.5	26.5	>600	130.5	145

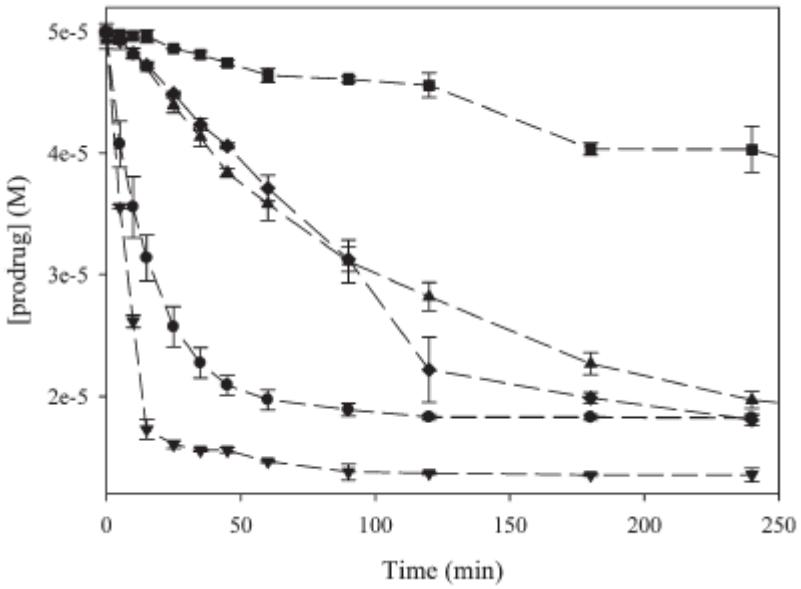

Figure 4. Hydrolysis of prodrugs in the presence of almond β-glucosidase ($1.0x10^{-6}$M) at 37°C (pH 7). GluClHQ (●), $GluCl_2HQ$ (▼), GluMeHQ (■), GluCQ (♦), GluOHQ (▲).

Biological activities

Antiproliferative activity. When analyzed for their antiproliferative activity against tumor A2780, A549 and MDA-MB-231 human cells, in the absence of Cu^{2+} ions, the investigated glycosides displayed discrete IC_{50}s that ranged from 4.1 μM to 55.3 μM (mean±SD, 26.2±17.8 μM), the exception being the glycoside GluMeHQ that displayed no activity (IC_{50}>100 μM) also in the presence of Cu^{2+} ion and, above all, compared to its not glycosylated counterpart (MeHQ, Table 4).

In the presence of 20 μM Cu^{2+} we observed a deep reduction of IC_{50}s for both the active compounds GluClHQ (mean reduction, 90±7%) and $GluCl_2HQ$ (mean reduction, 63±30%)(Table 4), with compound GluClHQ that displayed a higher mean antiproliferative activity compared to $GluCl_2HQ$ (2.04±2.23 μM vs 12.4±11.2 μM). A similar increase of activity in the presence of the Cu^{2+} ion and a similar ratio between the mean antiproliferative activity were also observed for the parent compounds ClHQ and Cl_2HQ (Table 4).

As regard to the target cell lines, the breast cancer cell line MDA-MB-231 was the less sensitive target for both glycosylated and not glycosylated compounds in most culture conditions.

Effect of the inhibition of glycosidase activity. As shown in Figure 5, the presence in culture conditions of the β-glycosidase inhibitor 2,5-dideoxy-2,5-imino-D-mannitol (DMDP) significantly increased the IC_{50} of both glycosylated compounds GluClHQ and $GluCl_2HQ$. As negative control we also evaluated the antiproliferative activity of not glycosylated ClHQ and Cl_2HQ compounds in the presence of DMDP. As expected in this case, no variation of the antiproliferative activity was observed demonstrating that glycosylated prodrugs may be activated only in the presence of an efficient β-glycosidase activity that releases the active 8-hydroxyquinoline moiety.

Table 4. Summary of IC_{50}s (μM) of glycosides and their parent compounds on A2780, A549 and MDA-MB-231 cells

	Cl_2HQ		$GluCl_2HQ$	
		Cu^{2+}		Cu^{2+}
A2780	24.64 ± 2.59[a]	2.53 ± 0.33	25.18 ± 2.22	3.12 ± 0.27
A549	23.87 ± 2.09	1.75 ± 0.49	31.97 ± 7.44	6.03 ± 1.37
MDA-MB-231	24.98 ± 3.15	4.97 ± 1.29	35.53 ± 3.09	28.12 ± 0.86
	ClHQ		GluClHQ	
		Cu^{2+}		Cu^{2+}
A2780	5.12 ± 0.94	0.47 ± 0.03	4.10 ± 0.47	0.36 ± 0.07
A549	5.93 ± 0.92	0.41 ± 0.20	5.32 ± 1.27	0.56 ± 0.03
MDA-MB-231	18.67 ± 5.89	0.59 ± 0.07	55.34 ± 4.98	5.20 ± 0.23
	MeHQ		GluMeHQ	
		Cu^{2+}		Cu^{2+}
A2780	8.46 ± 2.21	4.09 ± 0.23	>100	>100
A549	25.5 ± 3.12	4.66 ± 0.34	>100	>100
MDA-MB-231	50.65 ± 3.41	5.33 ± 0.15	>100	48.55 ± 2.18

[a] The numbers express the mean±SD of 4-8 data.

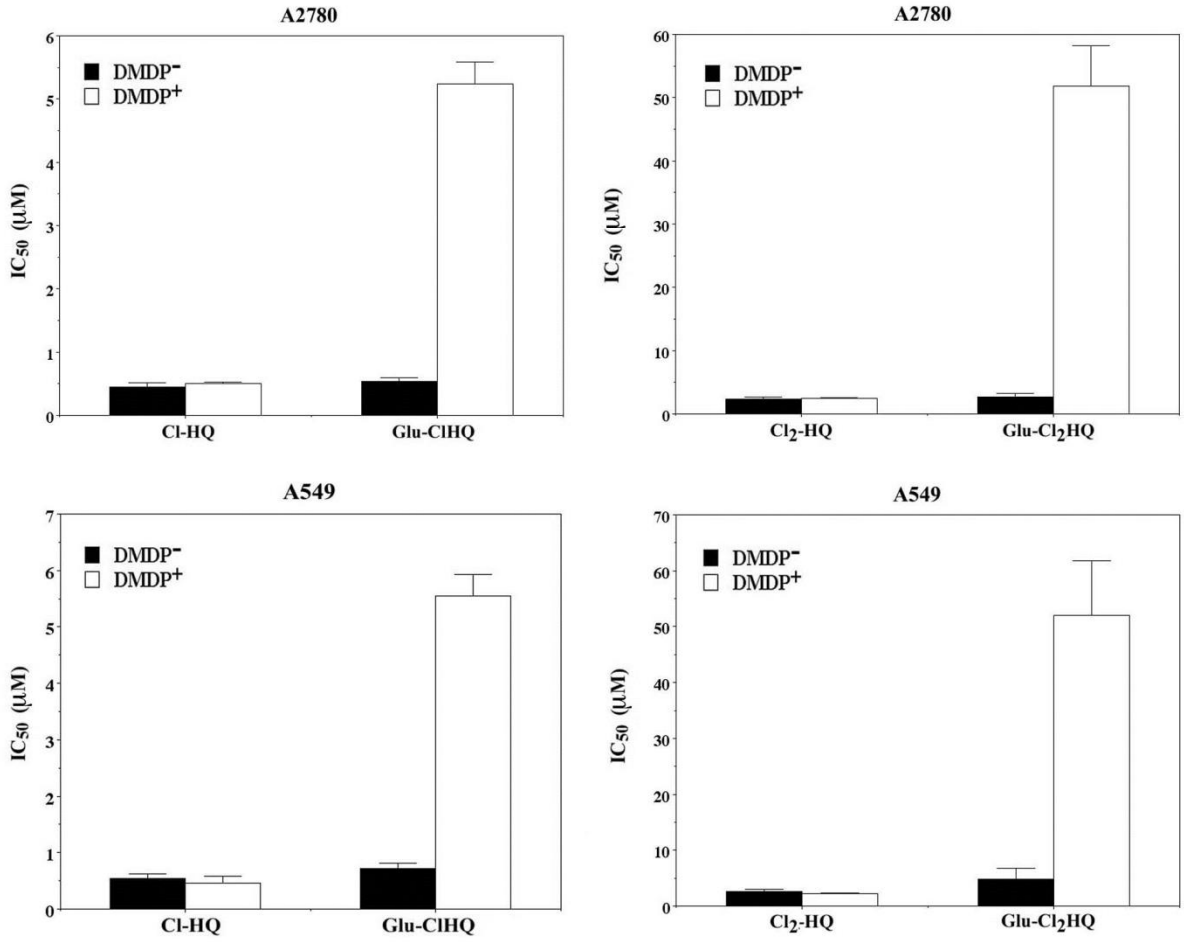

Figure 5. Histograms represent mean IC_{50}s of glucosylated and not glucosylated hydroxyquinolines in the presence or absence of the β-glucosidase inhibitor DMDP at 100 μM concentration.

Identification of apoptotic cells by DAPI and annexin V/PI stainings. Due to their pharmacologically significant antiproliferative activity both GluClHQ and $GluCl_2HQ$ and their not glycosylated parent compounds ClHQ and Cl_2HQ were analyzed by DAPI staining for the triggering of apoptosis. In general, the compounds showed a pharmacologically relevant apoptotic activity that was higher when the Cu^{2+} ions were present in culture. Compound Cl_2HQ represented an exception to this general rule in fact, at both equitoxic concentrations, we did not observe significant differences in terms of apoptotic cells in the presence or absence of Cu^{2+} ions (Table 5).
In order to confirm the previous data the GluClHQ and $GluCl_2HQ$ compounds were also analyzed for their ability to trigger apoptosis by the annexin V/PI staining. Once used at their IC_{50}s these

compounds confirmed the previous results obtained by the microscopy observation of nuclear morphology after DAPI staining. In particular, these results showed that a higher early and/or late apoptotic activity was developed in the presence of Cu^{2+} ions (Figure 6).

Table 5. Triggering of apoptosis by glucoconjugate compounds, as evaluated by nuclear morphological analysis after DAPI staining.

IC_{50}[a]								
	Cl_2HQ		$GluCl_2HQ$		ClHQ		GluClHQ	
		Cu^{2+}		Cu^{2+}		Cu^{2+}		Cu^{2+}
A2780	69.5 ± 26.1[b]	59.8 ± 16.2	14.5 ± 2.1	24.5 ± 0.7	5.8 ± 2.9	33.0 ± 13.9	7.0 ± 4.6	27.0 ± 13.8
A549	10.2 ± 6.2	7.3 ± 3.2	15.5 ± 4.2	38.4 ± 15.0	4.8 ± 3.9	14.2 ± 6.5	4.0 ± 2.0	22.6 ± 3.6
MDA-MB-231	2.8 ± 1.0	2.1 ± 1.8	2.3 ± 1.5	34.0 ± 12.2	3.0 ± 2.6	65.0 ± 7.0	3.0 ± 2.0	67.0 ± 4.7

[a] Each cell line was treated with the specific equitoxic concentrations IC_{50}, as calculated by the MTT assay.

[b] The means±SD (4-9 data) express the percentage of apoptotic cells.

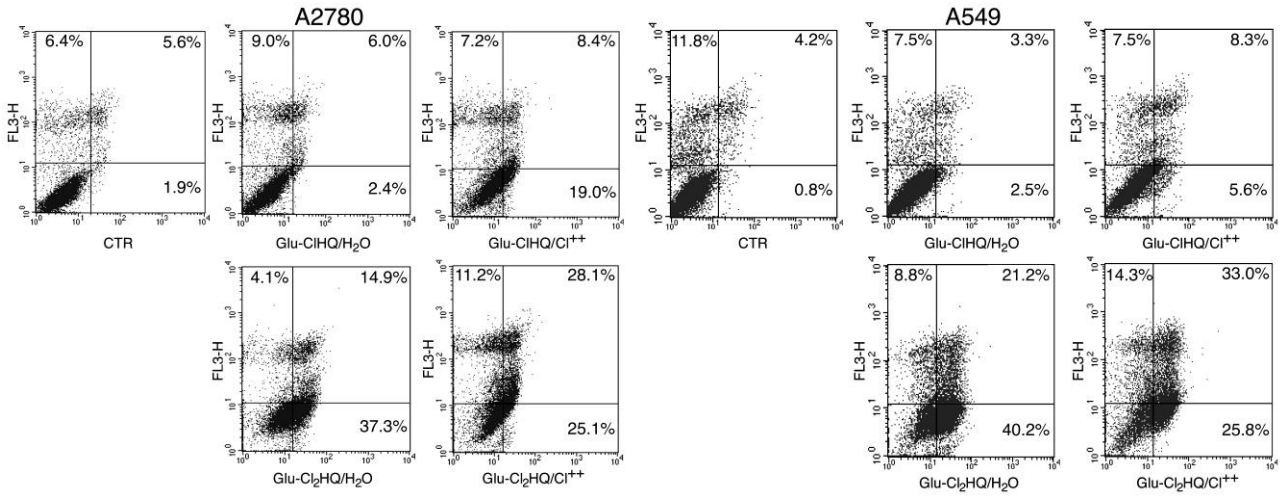

Figure 6. Scatter plots of A2780 and A549 cells labeled with Annexin-V/PI after three days culture in the presence of GluClHQ and $GluCl_2HQ$ in the presence or absence of Cu^{2+} ions.

Docking studies. The crystallographic structure of human cytosolic β-glucosidase[29] (hCBG, PDB code 2JFE, Figure 7A) shows that the active site of the enzyme is located on the bottom of a deep pocket (Figure 7B). It can be divided into two parts; the recognition site for the glucose moiety located at the bottom of the active site and the binding site for the aglycone at the entrance of the pocket. The active site is shaped as an oval or slit-like pocket with a cluster of hydrophobic amino acid sidechains (in yellow in Figure 7B) lining the walls of the aglycone binding slot, whereas hydrophobic, polar and charged residues are present in the glycone binding moiety.

2JFE provides useful 3D structural information for performing molecular docking studies. Investigated compounds were therefore docked to the binding cavity of 2JFE to evaluate their binding mode and affinity (kcal/mol).

To do that among the plethora of docking softwares, AutoDock Vina[30] was selected as main computational tool since it was recently used to model hydroxyquinolines in docking studies.[31] The performances of AutoDock Vina were evaluated by reproducing the crystal structure of the complex of the maize β-glucosidase (ZMGlu1) with the non-hydrolysable inhibitor p-nitrophenylbeta-D-thioglucoside (PDB code: 1E1F). In this validation step we paid particular attention to check the position of the glycone moiety at the bottom of the active site close to the two catalytic residues (Glu165 and Glu373 shown in Figure 7A for hCBG). The orientation of the glycone moiety of the substrate was in fact used as a filter to evaluatehCBG docking results. In particular, we retained the best poses of any ligand (= the most stable) provided that their glycone moiety was located at the bottom of the active site. This was verified for the three best poses of all compounds.

Results (Figure 7C-D) indicated that GluMeHQ has the best affinity for the binding site (-8.4 kcal/mol for the best pose), whereas $GluCl_2HQ$ shows the lowest affinity (-7.04 kcal/mol for the best pose). The three remaining compounds show intermediate values. FLAP[32] analysis confirmed this trend (data not shown).

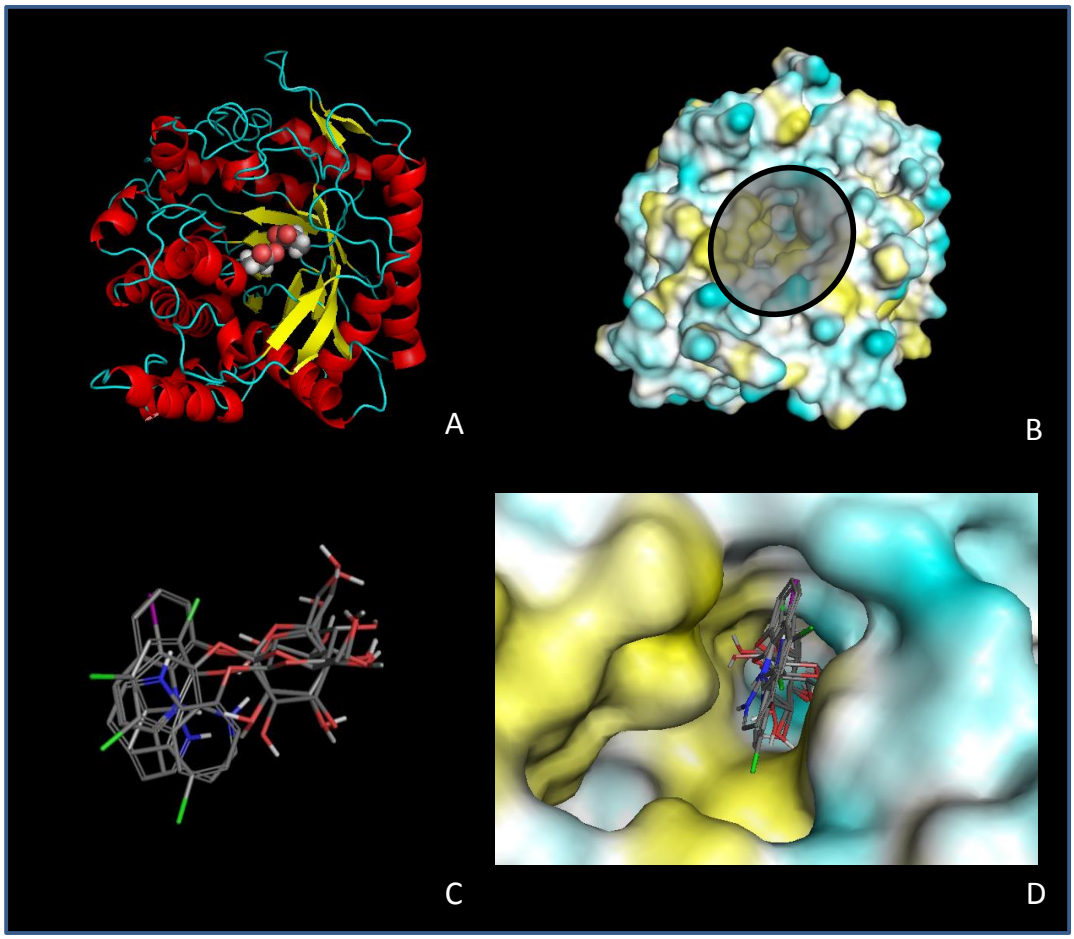

Figure 7. A) The crystallographic structure of human cytosolic β-glucosidase (hCBG, PDB code 2JFE); B) the active site of hCGB; the two catalytic residues (Glu165 and Glu373) are evidenced; C) The best poses of the five docked structures as obtained with AutoDock Vina abd; D) The best poses of the five docked structures in the active site (hydrophobic residues in yellow; hydrophilic residues in light blue).

Discussion

The main purpose of the study was the design of new compounds able to selectively target tumor cells exploiting some of their specific biochemical features.

Firstly, as known and described before, tumor cells have the unique characteristic of containing elevated copper concentrations.[33, 34]

Secondly, tumor cells express an altered carbohydrate metabolism that is characterized by an elevated glycolysis that in turn justifies the glucose avidity described in the 50s by Otto Warburg and generated the idea of the so-called "Warburg effect".[35] This concept implies that tumor cells, due to their glucose avidity, possess an increased glucose transport caused by an over-expression of the glucose transporters.[36,37]

Finally, Arafa[38] demonstrated that in the cancer cells used for his study the different β-glucosidase activity profiles well correlated with the cytotoxicity rank order of the glucosides object of his research. This demonstration underlines the important role that these enzyme activities could have for the bioactivation of glycosilated prodrugs. This concept was not entirely new since previously other authors had identified this mechanism as essential for the activation of their glycosilated compounds.[39,40,41] Taken together, all these works clearly demonstrate that the expression of the β-glucosidase or β-galactosidase activities is responsible for the bioactivation of the novel glycosilated prodrugs with the formation of the active aglycone moieties. Of course the level of expression of these enzymes into cancer cells remains an essential point distinguishing the pharmacological from the toxic effect of these compounds. On the whole a good balance between the β-glucosidase activity and the transmembrane glucose transporters may ensure the right and effective activation of glycosilated prodrugs[42]. In practice, high cellular β-glycosidase levels might be effective only when transport proteins are expressed as well.

An important future goal for the anticancer research is the oral administration of antitumor drugs that is expected to be accompanied by much greater patient tolerability and reduced associated cost. To reach this aim the application in the early stages of the drug discovery process

of knowledge of the compound's absorption, distribution, metabolism and excretion (ADME) profile is mandatory. In fact the optimization of the ADME profile is expected to significantly improve the candidates 'druggability'[43] and in fact few of the anticancer drugs currently in the clinic have optimized ADME features.[44] Also solubility issues should be taken into consideration. Here we designed compounds that are predicted to show drug-like physicochemical properties since they are all within the range set by Lipinski's Ro5. Moreover, prodrugs are predicted to be significantly more soluble than parent compounds. Finally, ADME *in silico* data predict a good pharmacokinetic profile at least for distribution and metabolism events.

GluClHQ, $GluCl_2HQ$ and GluMeHQ were synthetized in good yields with a straightforward procedure. The synthesis was optimized in order to obtain the pure β-anomer in a one-pot reaction. The β-anomers were the compounds of interest in this study because the tumor cells generally have a high expression of β-glucosidase. The desired products have been fully characterized by NMR, UV-Vis, CD, and ESI-MS. The purity of compounds has been confirmed by different techniques. The compounds were obtained pure without the use of elaborate processes of purification. This aspect is very important, considering one of the main reasons of CQ withdrawal from the market was the presence of di-iodo impurities. Furthermore, O-glycosylation of compounds masks the metal binding site, thereby preventing systemic chelation. This is the reason why the glucosides are not able to complex metal ions. The pyridine ring can complex copper(II) only with a log K_1 about 2.6[45], thus the glucose moiety has to be cleaved before efficient metal chelation of the quinolone ring.

ClHQ, Cl_2HQ and MeHQ are able to complex metal copper(II) with good stability constants,[45] forming CuL and CuL_2 as main species. The amount of each complex species depends on the concentration of copper(II) and the ligands.

We have already described[22] that the presence of Cu^{2+} ions makes glycosylated compounds more active in terms of antiproliferative activity than in culture conditions characterized by lower Cu^{2+} concentration. This difference is confirmed by present data where the presence of a high Cu^{2+}

concentration improved the activity of investigated derivatives by about ten times. The presence of a discrete activity in the absence of added Cu^{2+} ions may be ascribed to the possible high Cu^{2+} content of tumor cells utilized for our tests *in vitro*. It is also worth noting that ClHQ is the most active hydroxyquinoline of the series here studied, with IC_{50} ranging between 5.12±0.94 μM and 18.7±5.9 μM.

An important result of the study is finding that glycosilated compounds have an antiproliferative activity nearly similar to that of their parent compound except for the methyl derivative that showed a very low activity in all three cell lines used for our *in vitro* tests.

These data are consistent with the glucosidase cleavage assay *in vitro* and docking studies. Experimental cleavage studies suggest that the glucoconjugates are not hydrolyzed in the same way by glucosidase. In fact GluMeHQ, which results inactive in the antiproliferative assay, is the compound cleaved in longer times in comparison to the other glycosydes. These experimental results are supported by docking studies that show that prodrugs with high t1/2 are tighter bound to the active site than those with low $t_{1/2}$. This trend is verified by using two docking algorithms showing very different theoretical approaches and could suggest that compounds that are too tightly bound to the enzyme are slowly hydrolised. We are also aware that this relationship between experimental and computational data should be considered with caution for at least two reasons. Firstly, it is known that the active site of β-glucosidases is well-conserved, but here experimental and computational data were obtained using two different enzymes, almond glucosidase and hCBG, respectively. Secondly, it must be kept in mind that docking calculations can simulate only the recognition phase between enzyme and substrates and give no information on the whole enzymatic phenomenon.

As for the apoptosis, the opinion, initially quite controversial, that this death mechanism plays an essential role in the response to the chemotherapeutics,[46,47] has now been considered a landmark for anticancer drug research and for new chemotherapy-based procedures. It is well known that apoptosis represents, together with necrosis, an important pathway of cell death after

chemotherapy. Thus the evaluation of the triggering of apoptosis by the new compounds with anticancer activity becomes necessary both in *in vitro* and *in vivo* studies.[48,49] In the case of our glucoconjugates it is worth noting that their antiproliferative activity was always developed together with a significant triggering of this important and essential death event for chemotherapeutic agents and that this was in general higher when Cu^{2+} ions were added to the culture medium at equitoxic conditions of antiproliferative activity. The only exception to this rule is the use of Cl_2HQ where the presence of Cu^{2+} ions does not imply an increased apoptosis.

In order to verify that the glucosidase enzymatic activation of glucoconjugates is crucial for their antiproliferative activity we also performed antiproliferative experiments in the presence of Cu^{2+} ions and the known β-glucosidase inhibitor DMDP. Interestingly, the IC_{50}s of the most active glycosilated hydroxylquinolines GluClHQ and $GluCl_2HQ$, after treatment with DMDP, significantly increased by several times, while DMDP did not affect the activities of the parent compounds. These data unequivocally confirm the importance of the presence of β-glucosidase activity to allow the release of the active quinoline moiety in order to develop the antiproliferative activity after the binding of the Cu^{2+} ions.

The differences in sensitivity between the cell lines, in particular the lower sensitivity of the breast cancer cell line MDA-MB-231, could be interpreted on the basis of the absence of a sufficient number of glucose-transporters since the level of β-glucosidase (data not shown) were similar to those observed in the other two cell lines A2780 and A549. Opportune dosages of the concentration of membrane glucose-transporters could better explain our results.

A final point to be highlighted concerns the mechanism of action of OHQs as anticancer agents. In the last few years the ubiquitin-proteasome system (UPS) has emerged as a possible target for new anticancer compounds due to its involvement in the regulation and control of important protein in turn involved in vital cell mechanisms, such as proliferation, signal transduction, gene trascription, DNA repair and apoptosis.[50] The UPS acts in the turnover of proteins thanks to the involvement of tens of genes[51,52] some of which code enzymes working in

processes, such as the protein ubiquitination and deubiquitination with very specific mechanisms of targeting.[53] At present the bulk work on the UPS has led to the synthesis and clinical use of Bortezomib, an anticancer drug specific for the chymotripsin-like activity of proteasome whose inhibition seems to be directly involved in the induction of apoptosis in tumors,[54] which is mainly used in clinics for the treatment of myeloma.[55] Other hydroxyquinolines have as main mechanism of action the ability to interact with the UPS, in particular with the chymotripsin-like activity of proteasome, causing the arrest of the cell cycle and the triggering of apoptosis. The glycosilated compounds object of this study, by analogy, could have the same mechanism of action once deprived of the glucose moiety thanks to the action of β-glucosidase.

Conclusion

We designed and synthesized new glucoconjugates of OHQ derivatives built exploiting three frequent features of cancer cells, such as the high expression and content of β-glycosidase activity and Cu^{2+} concentration, and the high membrane concentration of glucose transporters linked to the "natural" glucose avidity of tumors. We show that these features can be synergistically combined to obtain new compounds highly specific for neoplastic cells. Physicochemical and ADME considerations were also included in the design phase of the project. The exploitation of these characteristics, all contained in a single molecule should, not only allow for a better selection of target tumor cells, but also minimize the chemotherapeutic side effects.

Experimental Section

Materials. Commercially available reagents were used directly, unless otherwise noted. 5-chloro-8-quinolinol (ClHQ), 5,7-dichloro-8-quinolinol (Cl_2HQ), 2-methyl-8-quinolinol (MeHQ) were purchased by Sigma-Aldrich. TLC was carried out on silica gel plates (Merck 60-F254). β-Glucosidase from almonds was obtained from Sigma-Aldrich.

NMR spectroscopy. ^{1}H and ^{13}C NMR spectra were recorded at 25°C with a Varian UNITY PLUS-500 spectrometer at 499.889 and at 125.7 MHz respectively. The NMR spectra were obtained by using standard pulse programs from Varian library. The 2D experiments (COSY, TOCSY, gHSQCAD. gHMBC) were acquired using 1K data points, 256 increments and a relaxation delay of 1.2 s.

Mass spectrometry, UV-vis and circular dichroism spectroscopy. The ESI-MS measurements were performed on a Finnigan LCQ-Duo ion trap electrospray mass spectrometer. The UV spectra were recorded using an Agilent 8452A diode array spectrophotometer. CD measurements were performed under a constant flow of nitrogen on a JASCO model J-810 spectropolarimeter. The spectra represent the average of 10 scans and were recorded at 25°C, on freshly prepared methanol solutions.

General procedure for the synthesis of the glucoconjugates. 8-Quinolinol derivative (0.75 mmol) and K_2CO_3 (7.5 mmol) were added to water (50 mL) and methanol (40 mL). Dichloromethane (100 mL) was added to this aqueous solution, followed by acetobromoglucose (1.88 mmol) and tetrabutylammonium bromide (0.75 mmol). The resulting mixture was vigorously stirred for 68 h. As for, ClHQ and Cl_2HQ, a solid precipitated, and the deacetylated products were collected by filtration, washed with cool methanol and dried. As for, MeHQ, the two-phase system was separated, and the aqueous phase was washed repeatedly with dichloromethane. The aqueous

phase was partially evaporated under vacuum to remove residual organic solvents and then a white solid precipitated. The product was collected by filtration washed with cool methanol and dried.

The purity was assayed by HPLC (Varian Prepstar instrument equipped with a Prostar 330 photodiode array detector. Column: Econosphere ODS (Alltech) column (5 μm, 2.0×250 nm), eluent: linear gradient water →CH_3CN).

5-chloro-8-quinolinyl-β-D-glucopyranoside (GluClHQ). Yield: 68%. TLC: Rf=0.51 (PrOH/AcOEt/H_2O/NH_3 4:4:1:1). HPLC Purity 98%.

ESI-MS: m/z=341.85 $[GluClHQ+H]^+$, 363.92 $[GluClHQ+Na]^+$, 704.61 $[2GluClHQ+Na]^+$

^{1}H NMR (500 MHz, CD_3OD) δ (ppm): 8.97 (dd, $J_{2,3}$ = 4.3, $J_{2,4}$ = 1.6 Hz, 1H, H-2), 8.71 (dd, $J_{4,3}$ = 8.6, $J_{4,2}$ = 1.6 Hz, 1H, H-4), 7.75 (dd, $J_{3,4}$ = 8.6, $J_{3,2}$ = 4.3 Hz, 1H, H-3), 7.67 (d, $J_{6,7}$ = 8.5 Hz, 1H, H-6), 7.51 (d, $J_{7,6}$ = 8.5 Hz, 1H, H-7), 5.09 (d, $J_{1,2}$= 7.8 Hz, 1H, H-1 of Glu), 3.97 (dd, $J_{6a,6b}$ = 12.1, $J_{6a,5}$=2.2 Hz, 1H, H-6a of Glu), 3.81 – 3.64 (m, 2H, H-2 and H-6b of Glu), 3.60-3-54 (m, 2H, H-3, H-5), 3.45 (dd, J = 9.6, 9.0 Hz, 1H, H-4).

^{13}C NMR (125 MHz, CD_3OD) δ (ppm): 153.2 (C-8), 151.1 (C-2), 140.9 (C-9), 135.1 (C-4), 128.4 (C-6, C-5), 125.0 (C-10), 124.1 (C-3), 114.5 (C-7), 103.3 (C-1 of Glu), 78.6 (C-5 of Glu), 77.4 (C-3), 74.7 (C-2 of Glu), 71.6 (C-4 of Glu), 63.0 (C-6 of Glu).

UV-Vis: (CH_3OH) λ/nm (ε): 243 (25600), 317 (3360).

CD (CH_3OH) λ/nm (Δε): 197.8 (-4.24), 311.4 (-0.70).

Elemental analysis for $C_{15}H_{16}NClO_6 \cdot H_2O$: calc. C 50.06; H 5.05; N 3.89; found C, 50.00; H, 4.99; N, 3.94.

5,7-dichloro- 8-quinolinyl-β-D-glucopyranoside ($GluCl_2HQ$). Yield: 61%. TLC: Rf=0.52 (PrOH/AcOEt/H_2O/NH_3 4:4:1:1). HPLC Purity 98%. ESI-MS: m/z=375.85 $[GluCl_2HQ+H]^+$, 397.92 $[GluCl_2HQ+Na]^+$, 772.51 $[2GluCl_2HQ+Na]^+$.

^{1}H NMR (500 MHz, CD_3OD) δ (ppm): 8.98 (dd, $J_{2,3}$ = 4.3Hz, $J_{2,4}$ = 1.5 Hz, 1H, H-2), 8.68 (dd, $J_{4,3}$ = 8.6, $J_{4,2}$ = 1.6 Hz, 1H, H-4), 7.82 (s, 1H, H-6), 7.72 (dd, $J_{3,4}$ = 8.6, $J_{3,2}$ = 4.3 Hz, 1H, H-3), 5.34 (d, $J_{1,2}$ = 7.8 Hz, 1H, H-1 of Glu), 3.77 (dd, $J_{6a,6b}$ =11.9, $J_{6a,5}$= 2.4 Hz, 1H, H-6a), 3.72 (dd, $J_{2,3}$ = 8.8, $J_{2,1}$ = 7.8 Hz, 1H, H-2), 3.66 (dd, $J_{6b,6a}$ = 11.9, $J_{6b,5}$= 5.3 Hz, 1H, H-6b) 3.50 – 3.42 (m, 2H, H-4, H-3), 3.23 (ddd, $J_{5,4}$ = 9.4, $J_{5,6b}$ = 5.3, $J_{5,6a}$ = 2.3 Hz, 1H, H-5).

^{13}C NMR (125 MHz, CD_3OD) δ (ppm): 152.3 (C-2), 143.4 (C-8), 144.1 (C-9), 135.6 (C-4), 130.0 (C-6), 129.2 (C-7), 128.5 (C-5), 127.8 (C-10), 124.2 (C-3), 107.3 (C-1 of Glu), 78.6 (C-5 of Glu), 78.4 (C-3), 72.2 (C-2 of Glu), 71.3 (C-4 of Glu), 62.7 (C-6 of Glu).

UV-Vis (CH_3OH) λ/nm (ε) : 207 (20900), 242 (24800), 302 (3020).

CD (CH_3OH) λ/nm (Δε): 206.6 (-5.10), 240.2 (-10.77), 318.0 (0.73).

Elemental analysis for $C_{15}H_{15}NCl_2O_6 \cdot H_2O$: calc. C 45.68; H 4.35; N 3.55; found C, 45.59; H, 4.30; N, 3.58.

2-methyl-8-quinolinyl-β-D-glucopyranoside (GluMeHQ). Yield: 57%. TLC: Rf=0.44 (PrOH/AcOEt/H_2O/NH_3 4:4:1:1). HPLC Purity 98%. ESI-MS: m/z= 321.94 $[GluMeHQ+H]^+$, 344.00 $[GluMeHQ+Na]^+$ 359.87 $[GluMeHQ+K]^+$ 664.61 $[2GluMeHQ+Na]^+$, 680.80 $[2GluMeHQ+K]^+$.

^{1}H NMR (500 MHz, CD_3OD) δ (ppm): 8.24 (d, $J_{4,3}$ = 8.4 Hz, 1H, H-4), 7.56 (dd, $J_{5,6}$ = 6.8, $J_{5,7}$ = 2.7 Hz, 1H, H-5), 7.48 (m, 3H, other aromatic H), 5.05 (d, 1H, $J_{1,2}$= 7.8. Hz, H-1 of Glu), 3.96 (dd, 1H, $J_{6a,6b}$ = 12.1, $J_{6a,5}$ = 2.2 Hz, H-6a of Glu), 3.75 (dd, 1H, $J_{6a,6b}$ = 12.1, $J_{6b,5}$ = 15.0 Hz, H-6b of Glu), 3.73 (t, 1H, H-2 of Glu), 3.56 (m, 2H, H-5 and H-3 of Glu), 3.46 (t, 1H, $J_{4,3}$ =$J_{4,5}$ = 18 Hz, H-4 of Glu), 2.77 (s, 3H, CH_3).

^{13}C NMR (125 MHz, CD_3OD) δ (ppm): 154.5 (C-2), 148.0 (C-8), 133.2 (C-9), 134.7 (C-4), 123.6 (C-6, C-10), 120.3 (C-3), 118.9 (C-5), 111.5 (C-7), 105.3 (C-1 of Glu), 77.0 (C-3 and C-5 of Glu), 74.7 (C-2 of Glu), 69.8 (C-4 of Glu), 61.2 (C-6 of Glu), 20.8 (CH_3).

UV-Vis (CH_3OH) λ/nm (ε): 204 (31700), 240 (32200), 297 (3110).

CD (CH_3OH) λ/nm (Δε): 196.8 (-2.68), 312.6 (-0.34).

Elemental analysis for $C_{15}H_{15}NO_6 \cdot H_2O$: calc. C 56.62; H 6.24; N 4.13; found C, 56.65; H, 6.21; N, 4.09.

Copper(II) complex studies. The copper(II) complexes were prepared by adding a solution of $CuSO_4$ to a ligand solution in 1:1 ratio. ClHQ and Cl_2HQ are poorly soluble in water and their metal complexes were examined in a methanol/water mixture (80/20 w/w).

All the ESI-MS measurements were carried out by using a Finnigan LCQ DECA XP PLUS ion trap spectrometer operating in the positive ion mode and equipped with an orthogonal ESI source (Thermo Electron Corporation, USA). Sample solutions were injected into the ion source without the addition of any other solvent at a flow rate of 5 μL/ min. For electrospray ionization the drying gas (N_2) was heated at 270 °C. The capillary exit and skimmer voltage were varying in order to optimize the signal responses. Scanning was performed from m/z=100 to 2000 and no fragmentation processes were observed under our experimental conditions. Xcalibur software was used for the elaboration of mass spectra. Each species is indicated with the m/z value of the first peak of its isotopic cluster.

***In vitro* stabilities of glucoconjugates.** The three final compounds were incubated at 37° C in PBS to monitor their stabilities by TLC, ESI-MS and UV-Vis spectroscopy. Furthermore, the compound stability was monitored at pH 4 and 11.

Enzymatic cleavage assay. Glycoconjugates were incubated at 37 °C for 2 h. TLC and ESI-MS monitoring of the glucosidase reactions were used to determine whether the clioquinol glycosides showed any sign of being cleaved by the enzyme. Enzymatic cleavage was also monitored by UV-vis spectroscopy. Unless stated otherwise, β-glucosidase (1.0×10^{-6} M) was incubated in the assay solution in the presence of the glycoconjugates (5.0×10^{-5} M) at 37 °C. Samples (2 mL) were

removed at selected time points over 4h and were immediately added with a solution of NaOH until the pH value of the solution reached 11.0 in order to stop enzymatic activity. Furthermore at this pH the released drug show a shift of the bands because of the deprotonation of phenolic group and so it is possible to quantify the released drug through UV-vis spectroscopy. Calibration curves of the free ligands for absorbance against their concentrations were obtained at pH 11.0. The UV-vis spectra were recorded in 1.0 cm path length matched quartz cuvettes with an Agilent 8452A diode array spectrophotometer at 37 °C. All assays were performed in triplicate.

Dilution of glycosides and parent compounds for biological determinations. All glycosides and parent compounds were firstly dissolved in 100% dimethylsulfoxide (DMSO) at the concentration of 100 mM and then further diluted in fetal calf serum (FCS, final concentration DMSO 0.2-0.4%).

Determination of antiproliferative activity by the MTT assay. Human cell lines A549 (lung, carcinoma), A2780 (ovary, adenocarcinoma), and MDA-MB-231 (breast, carcinoma) were plated at 10^5/ml, 0.89 x 10^5/mL and 2 X 10^5/mL, respectively, in 180 μl complete medium into flat-bottomed 96-well microtiter plates. After 6-8 hours cells were treated with 20 μl containing five 1:10 fold concentrations of our compounds diluted in FCS containing 2% or 4% DMSO in the presence or absence of $CuCl_2$ salt (20 μM). After 72 hours plates were processed and IC_{50}s values calculated as described elsewhere.[56] Each experiment was repeated 4-8 times.

Inhibition of glucosidase activity. The evaluation of antiproliferative activity was performed on A2780 and A549 cells in the presence of Cu^{2+} ions and 100 μM of the β-glycosidase inhibitor 2,5-dideoxy-2,5-imino-D-mannitol (DMDP). The same experiments were carried out without DMDP as a control.

Microscopy visualization of apoptotic cells after 4'-6-diamidino-2-phenylindole (DAPI) staining. A2780, A549 and MDA-MB-231 were plated in 24-well plates at their optimal densities/well (see above) in 1 ml complete medium for 6-8 h. ClHQ, Cl_2HQ and their glycosylated counterparts were then added to obtain their specific final IC_{50}, as determined by the MTT assay. After 72 hours floating and adherent cells were harvested, washed twice with cold PBS, fixed with 60 μL of 70% ethanol in PBS and maintained at 4 °C until analysis. For microscopy examination 5 μL of 10 μg/ml DAPI in water were added to the samples, and the percentage of apoptotic segmented nuclei/cells evaluated.

Evaluation of apoptosis by annexin-V/PI staining. The triggering of apoptosis was also evaluated for the glycosylated compounds Glu-ClHQ and Glu-Cl_2HQ in A2780, and A549 cells. Cells were treated with the specific IC_{50} of each compound in the presence or absence of Cu^{++} salt (20 μM). Three days after floating and adherent cells were harvested, washed with cold PBS and early and late apoptotic cells determined by double staining with FITC-annexin-V/PI (rh Annexin-V/FITC Kit, Bender MedSystem GmbH, Vienna, Austria). The subsequent analysis was performed by flow cytometry as described elsewhere.[57]

Physicochemical and ADME profile. Solubility (expressed as ALOGpS, the higher, the more soluble the compound) was calculated with VCCLAB, Virtual Computational Chemistry Laboratory, http://www.vcclab.org, 2005.[58] The conformational hypersurface of compounds was explored with the standard conformational search module implemented in MOE2009.10. Virtual log P calculations were performed with VEGA ZZ 3.0.0 (http://www.vegazz.net).

The 3D structures (see below) were submitted to VolSurf+ (version 1.0.4, Molecular Discovery Ltd. Pinner, Middlesex, UK, 2009, http://www.moldiscovery.com)[59] using default settings and four probes (OH2, DRY N1 and O probes that mimic respectively water, hydrophobic, hydrogen bond

acceptor and hydrogen bond donor interaction of the compounds with the environment). The molecules were projected on the pre-calculated models implemented in VolSurf+ to calculate Ro5 and ADME parameters.

Molecular docking. The crystal structure of human cytosolic β-glucosidase was obtained from the RCSB Protein Data Bank, code 2JFE. The 3D structure was visualized and modified with Pymol v1.1.r1 as follows. Water and NAG molecules were removed, hydrogen atoms were added and the resulting structure was saved in the pdb format. Ligands were built using CORINA[60] and saved in the mol2 format. AutoDock Vina[30] and FLAP UI version 0.43.0[32] were used to perform docking studies. The active site in AutoDock was defined by the coordinates of Cα of the catalytic residue Glu165 (33 (X), 51 (Y) and 38 (Z)).[29] To ensure a correct docking process, the search space was defined to encompass all flexible residues as a box with dimensions of 30.0 × 30.0 × 30.0 Å. Ligand Explorer v.3.9 was used to visualize the interactions of bound ligands in the protein.

Statistical analysis. The Mann-Whitney test for non-parametric data was used for the statistical analysis of data.

Acknowledgements. We thank MIUR [2008R23Z7K, PRIN 2008F5A3AF, FIRB2010_RBAP114AMK and RBNB08HWLZ (Merit)] for the financial support. We thank Tiziana Campagna for her technical assistance.

Supporting Information. ^{1}H NMR spectra (COSY, TOCSY, HMQC, HSQC), ^{13}C NMR spectra and MS-ESI spectra for all prodrugs. UV-Vis spectra used for kinetic experiments.

Abbreviations used. CQ, clioquinol; OHQ, 8-hydroxyquinoline; AD, Alzheimer Disease; GLUT, glucose transporter; ADME, absorption, distribution, metabolism and excretion; CD, circular

dichroism; TLC, thin layer chromatography; DMDP, 2,5-dideoxy-2,5-imino-D-mannitol; DMSO, dimethylsulfoxide; PBS, phosphate buffered saline, FCS, fetal calf serum; DAPI, 4'-6-diamidino-2-phenylindole; UPS, ubiquitin-proteasome system; MTT, 3-(4,5-dimethythiazol-2-yl)-2,5-diphenyl tetrazolium bromide; hCBG, human cytosolic β-glucosidase.

References

(1) Jemal, A.; Siegel, R.; Xu, J.; Ward, E. Cancer Statistics, 2010. *CA Cancer J. Clin.,* **2010**, 60, 277–300.

(2) Jemal, A.; Bray, F.; Center, M. M.; Ferlay, J.; Ward, E.; Forman, D. Global Cancer Statistics. *CA Cancer J. Clin.,* **2011**, 61, 69–90.

(3) Hung L. W. H.; Barnham J. K. Modulating metals as a therapeutic strategy for Alzheimer's disease. *Future Med. Chem*. **2012**, 4, 955-969.

(4) Yassin, M. S.; Ekblom, J.; Xilimas, M.; Gottfries C. G. Changes in uptake of vitamin B12 and trace metals in brains of mice treated with clioquinol. *J. Neurol. Sci.* **2000**, 173, 40-44.

(5) http://clinicaltrials.gov/ct2/show/study/NCT00963495

(6) Zhai, S.; Yang, L.; Cui, Q. C.; Sun, Ying; D., Q. P.; Yan, B. Tumor cellular proteasome inhibition and growth suppression by 8-hydroxyquinoline and clioquinol requires their capabilities to bind copper and transport copper into cells. *J. Biol. Inorg. Chem*. **2010**, 15, 259–269.

(7) Banci, L.; Bertini, I.; Cantini, F.; Ciofi-Baffoni, S. Cellular copper distribution: a mechanistic systems biology approach. *Cell. Mol. Life Sci.* **2010**, 67, 2563-2589.

(8) Brem, S. Angiogenesis and cancer control: from concept to therapeutic trial. *Cancer Control.* **1999**, 6, 436–458.

(9) Brewer, G.J. Copper control as an antiangiogenic anticancer therapy: lessons from treating Wilson's disease. *Exp. Biol. Med.* **2001**, 226, 665–673.

(10) Pass, H.I.; Brewer, G.J.; Dick, R.; Carbone, M.; Merajver, S. A phase II trial of tetrathiomolybdate after surgery for malignant mesothelioma: final results. *Ann. Thorac. Surg.* **2008**, 86, 383-389.

(11) Henry, N.L.; Dunn, R.; Merjaver, S.; Pan, Q.; Pienta, K.J.; Brewer, G.; Smith, D.C. Phase II trial of copper depletion with tetrathiomolybdate as an antiangiogenesis strategy in patients with hormone-refractory prostate cancer. *Oncology* **2006,** 71, 168-175.

(12) Brewer, G.J.; Askari, F.; Dick, R. B.; Sitterly, J.; Fink J. K.; Carlson, M.; Kluin, K.J.; Lorincz, M.T. Treatment of Wilson's disease with tetrathiomolybdate: V. Control of free copper by tetrathiomolybdate and a comparison with trientine. *Transl. Res*. **2009**, 154, 70-77.

(13) Duncan C., White A.R. Copper Complexes as therapeutic agents. *Metallomics* DOI 1'.1039/c2mt00174h.

(14) Schimmer, A. D. Clioquinol- A novel copper-dependent and independent proteasome inhibitor. *Curr. Cancer Drug Targets* **2011**, 11, 325-331.

(15) Milacic, V.; Jiao, P.; Zhang, B.; Yan, B; Dou, Q. P. Novel 8-hydroxylquinoline analogs induce copper-dependent proteasome inhibition and cell death in human breast cancer cells. *Int. J. Oncol.* **2009**, 35, 1481-1491.

(16) Cater, M.A.; Haupt, Y. Clioquinol induces cytoplasmic clearance of the X-linked inhibitor of apoptosis protein (XIAP): therapeutic indication for prostate cancer. *Biochem. J*. **2011**, 436, 481-491.

(17) Katsuyama, M.; Iwata, K.; Ibi, M.; Matsuno, K.; Matsumoto, M.; Yale-Nishimura, C. Clioquinol indices DNA double-strand breaks, activation of ATM, and subsequent activatin of p53 signaling. *Toxicology* **2012**, 299, 55-59.

(18) Palombo,M.; Sinko, P. J.; Singh, Y. Recent Trends in Targeted Anticancer Prodrug and Conjugate Design. *Curr. Med. Chem.* **2008**, 15, 1802–1826.

(19) Nishioka, T.; Oda, Y.; Seino, Y.; Yamamoto, T.; Inagaki, N.; Yano, H.; Imura, H.; Shigemoto, R.; Kikuchi, H. Distribution of the glucose transporters in human brain tumors. *Cancer Res.* **1992**, 52, 3972-3979.

(20) Carvalho, K. C.; Cunha, I.W.; Rocha, R. M.; Ayala, F. R.; Cajaíba, M.M.; Begnami, M. D; Vilela, R. S.; Paiva, G. R.; Andrade, R. G.; Soares, F.A. GLUT1 expression in malignant tumors and its use as an immunodiagnostic marker. *Clinics* (Sao Paulo) **2011**, 66, 965–972.

(21) Cheng, H.; Cao,X.; Xian, M.; Fang, L.; Cai, T. V. Ji, J.J.; Tunac, J.B. Sun, D.; George Wang P. G. Synthesis and Enzyme-Specific Activation of Carbohydrate-Geldanamycin Conjugates with Potent Anticancer Activity. *J. Med. Chem.* **2005,** *48,* 645-652.

(22) Oliveri, V.; Giuffrida, M.L.; Vecchio, G.; Aiello, C.; Viale M. Gluconjugates of 8-hydroxyquinolines as potential anti-cancer prodrugs. *Dalton Trans.* **2012**, *41*, 4530-4535.

(23) Han van de Waterbeemd, H. Improving Compound Quality through in vitro and in silico Physicochemical Profiling. *Chem. Biodivers.* **2009**, *6*, 1760–1766.

(24) Gaillard P.; Carrupt, P.A.; Testa, B.; Boudon, A. Molecular Lipophilicity Potential, a tool in 3D QSAR: Method and applications. *J. Comput. Aid. Mol. Des.* **1994**, *8*, 83-96.

(25) Carosati, E.; R. Budriesi, R.; P. Ioan, P.; Ugenti, M.P.; Frosini, M.; Fusi, F.; Corda, G.; Cosimelli, B.; Spinelli, D.; Chiarini, A.; Cruciani, G. Discovery of Novel and Cardioselective Diltiazem- like Calcium Channel Blockers via Virtual Screening. *J. Med. Chem.* **2008**, *51*, 5552-5565.

(26) Mimaki, Y.; Watanabe, K.; Ando, Y.; Sakuma, C.; Sashida, Y.; Furuya, S.; Sakagami, H. Flavonol glycosides and steroidal saponins from the leaves of Cestrum nocturnum and their cytotoxicity. *J. Nat. Prod.* **2001**, *64*, 17-22.

(27) Rodger, A.; Norden, B. Circular Dichroism and Linear Dichroism. Oxford University Press New York **1997**.

(28) Budimir, A.; Humbert, N.; Elhabiri, M.; Osinska, I.; Birus, M.; Albrecht-Gary, A-M. Hydroxyquinoline based binders: Promising ligands for chelatotherapy. *J. Inorg. Biochem.* **2011**, *105*,490-496.

(29) Tribolo, S.; Berrin, J.-G.; Kroon, P.A.; Czjzek, M.; Juge, N. The crystal structure of human cytosolic β-glucosidase unravels the substrate aglycone specificity of a family 1 glycoside hydrolase. *J Mol. Biol.* **2007,** *370*, 964-975.

(30) Trott, O.; Olson, A. J. AutoDock Vina: improving the speed and accuracy of docking with a new scoring function, efficient optimization and multithreading. *J. Comput. Chem.* **2010**, *31*, 455-461.

(31) Bruyère, C.; Madonna, S.; Van Goietsenoven, G.; Mathieu, V.; Dessolin, J.; Kraus, J.-L.; Lefranc, F.; Kiss, R. JLK1486, a Bis 8-Hydroxyquinoline–Substituted Benzylamine, Displays Cytostatic Effects in Experimental Gliomas through MyT1 and STAT1 Activation and, to a Lesser Extent, PPARg Activation. *Transl. Oncol.* **2011**, *4*, 126–137.

(32) Cross, S.; Baroni, M.; Carosati, E.; Benedetti, P.; Clementi, S. FLAP: GRID Molecular Interaction Fields in Virtual Screening. Validation using the DUD Data Set. *J. Chem. Inf. Model.* **2010**, 50, 1442–1450.

(33) Geraki, K.; Farguharson, M.J.; Bradley, D.A. Concentrations of Fe, Cu and Zn in breast tissue: a synchrotron XRF study. *Phys Med Biol* **2002**, 47, 2327-2339.

(34) Diez, M.; Arroyo, M.; Cerdan, F.J.; Munoz, M.; Martin, M.A.; Balibrea, J.L. Serum and tissue trace metal levels in lung cancer. *Oncology* **1989**, 46, 230-234.

(35) Young, C.D.; Anderson, S.M. Sugar and fat - that's where it's at: metabolic changes in tumors. *Breast Cancer Res.* **2008**, *10*, 202-211.

(36) Nishioka, T.; Oda, Y. ; Seino, Y.; Yamamoto, T.; Inagaki, N.; Yano, H.; Imura, H.; Shigemoto R.; Kikuchi, H. Distribution of the Glucose Transporters in Human Brain Cancer *Cancer Res.* **1992**, *52*, 3972-3979.

(37) Kawamura, T.; Kusakabe, T.; Sugino, T.; Watanabe, K.; Fukuda, T.; Nashimoto, A.; Honma K., Suzuki, T. Expression of glucose transporter-1 in human gastric carcinoma: association with tumor aggressiveness, metastasis, and patient survival. *Cancer* **2001**, *92*, 634-641.

(38) Arafa, H. M.M. Possible contribution of β-glucosidase and caspases in the cytotoxicity of glufosfamide in colon cancer cells. *Eur. J. Pharmacol.* **2009**, *616*, 58–63.

(39) Syrigos, K. N.; Rowlinson-Busza, G.; Epenetos, A. A. In vitro cytotoxicity following specific activation of amygdalin by betaglucosidase conjugated to a bladder cancer-associated monoclonal antibody. *Int. J. Cancer* **1998**, 78, 712–719.

(40) Seker, H.; Bertram, B.; Troster, H.; Fisher, R.; Trendelenburg, M.; Wiessler, M. Potential influence of β-glucosidases on in vitro cytotoxicity mediated by β-D-Glc-IPM (glufosfamide), a new tumor therapeutic agent. *Annu. Meet Am Assoc. Cancer Res.* **2000**, 41, 602-603.

(41) De Graaf, M.; Pinedo, H. M.; Quadir, R.; Haisma, H.J.; Boven, E. Cytosolic beta-glycosidases for activation of glycoside prodrugs of daunorubicin. *Biochem. Pharmacol.* **2003**, 65, 1875–1881.

(42) Nomoto, M.; Yamada, K.; Haga, M.; Hayashi, M. Improvement of intestinal absorption of peptide drugs by glycosylation: transport of tetrapeptide by the sodium iondependent D-glucose transporter. *J. Pharm. Sci.* **1998**, 87, 326–332.

(43) Owens, J.; |Determining druggability. *Nat. Rev. Drug. Discov.* **2007**, *6*, 187-187.

(44) Daisy, P.; Suveena, S. Solutions to pharmaceutical issues for anticancer drugs by accord excel. *Asian J. Pharm. Clin. Res.* **2012**, *5*, 149-158.

(45) Martell, A. E.; Smith, R. M. Critical Stability Constants, Plenum, New York, **1977**.

(46) Fuster J.J.; Sanz-González S.M.; Moll U.M.; Andrés, V. Classic and novel roles of p53: prospects for anticancer therapy. *Trends Mol. Med.* **2007**, *13*, 192−199.

(47) Gadducci A.; Cosio S.; Muraca S.; Genazzani A.R. Molecular mechanisms of apoptosis and chemosensitivity to platinum and paclitaxel in ovarian cancer: biological data and clinical implications. *Eur. J. Gynaecol. Oncol.* **2002**, *23*, 390−396.

(48) Lerma-Díaz J.M.; Hernández-Flores G.; Domínguez-Rodríguez J.R.; Ortíz-Lazareno P.C.; Gómez-Contreras P, Cervantes-Munguía R, Scott-Algara D, Aguilar-Lemarroy A, Jave-Suárez L.F.; Bravo-Cuellar A. In vivo and in vitro sensitization of leukemic cells to adriamycin-induced apoptosis by pentoxifylline. Involvement of caspase cascades and IkappaBalpha phosphorylation. *Immunol. Lett.* **2006**, *103*,149−158.

(49) Yoshimoto Y, Kawada M, Ikeda D, Ishizuka M Involvement of doxorubicin-induced Fas expression in the antitumor effect of doxorubicin on Lewis lung carcinoma in vivo. *Int. Immunopharmacol.* **2005**, *5*, 281−288

(50) Yang, Y.; Kitagaki, J.; Wang, H.; Hou, D.; Perantoni, A. O. Targeting the ubiquitin-proteasome system for cancer therapy. *Cancer Sci.* **2009**, 100, 24–28.

(51) Vembar, S.S.; Brodsky, J.L. One step at a time: endoplasmic reticulum-associated degradation. *Nat. Rev. Mol. Cell. Biol.* **2008**, 9, 944-957.

(52) Ron, D.; Walter, P. Signal integration in the endoplasmic reticulum unfolded protein response. *Nat. Rev. Mol. Cell. Biol.* **2007**, *8*, 519-529.

(53) Liu, Y.; Ye, Y. Proteostasis regulation at the endoplasmic reticulum: a new perturbation site for targeted cancer therapy. *Cell. Research* **2011**, *21*, 867-883.

(54) An, B.; Goldfarb, R.H.; Siman, R. Dou, Q.P. Novel dipeptidyl proteasome inhibitors overcome Bcl-2 protective function and selectively accumulate the cyclin-dependent kinase inhibitor p27 and induce apoptosis in transformed, but not normal, human fibroblasts. *Cell Death Differ.* **1998**, 5, 1062–1075.

(55) Leonard, J.P.; Furman, R. R.; Coleman, M. Proteasome inhibition with bortezomib: a new therapeutic strategy for non-Hodgkin's lymphoma. *Int. J. Cancer* **2006**, 119, 971–979.

(56) Cafaggi, S.; Russo, E.; Stefani, R.; Leardi, R.; Caviglioli, G.; Parodi, B.; Bignardi, G.; De Totero, D.; Aiello, C.; Viale, M. Preparation and evaluation of nanoparticles made of chitosan or N-trimethyl chitosan and a cisplatin-alginate complex. *J. Control. Release* **2007**, 121, 110-123.

(57) Viale, M.; Cordazzo, C.; de Totero, D.; Budriesi, R.; Rosano, C.; Leoni, A.; Ioan, P.; Aiello, C.; Croce, M.; Andreani, A.; Rambaldi, M.; Russo, P.; Chiarini, A.; Spinelli, D. Inhibition of MDR1 activity and induction of apoptosis by analogues of nifedipine and diltiazem: an in vitro analysis. *Invest. New Drugs* **2011**, 29, 98-109.

(58) Tetko, I. V.; Gasteiger, J.; Todeschini, R.; Mauri, A.; Livingstone, D.; Ertl, P.; Palyulin, V. A.; Radchenko, E. V.; Zefirov, N. S.; Makarenko, A. S.; Tanchuk, V. Y.; Prokopenko, V. V. Virtual computational chemistry laboratory - design and description, *J. Comput. Aid. Mol. Des*., **2005**, *19*, 453-463.

(59) Cruciani,G.; Crivori, P.; Carrupt, P.; Testa, B. Molecular fields in quantitative structure – permeation relationships: the Volsurf+ approach. *J. Mol. Struct.(THEOCHEM),* **2000**, *503*, 17-30.

(60) http://www.molecular-networks.com/node/1